Characterization of Optical Redistribution Loss Developed for Co-Packaged Optics

Akihiro Noriki, Isao Tamai, Yasuhiro Ibusuki, Akio Ukita, Satoshi Suda, Koichi Takemura, *Member, IEEE*, Daisuke Shimura, *Member, IEEE*, Yosuke Onawa, Hiroki Yaegashi, and Takeru Amano

***Abstract*— We previously proposed a new package substrate called active optical package (AOP) substrate to realize co-packaged optics. An optical redistribution technology on silicon photonics dies was developed to fabricate the AOP substrate. It is composed of a polymer waveguide, with a mirror-based optical coupling between the polymer and silicon waveguides. The fabricated optical redistribution loss was characterized in this study. An average loss of approximately 4 dB and wavelength dependent loss of ±1 dB were observed for the wavelength range of 1460–1600 nm. It was shown that the low wavelength-dependent optical redistribution was available owing to the broadband characteristics of mirror-based optical coupling and polymer waveguide.**

***Index Terms*— Co-packaged optics, micro mirror, optical redistribution, polymer waveguide, silicon photonics.**

I. Introduction

DATA movement in high-performance computer systems and large-scale data centers is a critical concern [1]. Increasing the data rates of conventional electrical links leads to low latency tolerance, high power consumption, and poor signal integrity, particularly for long-distance interconnects. Co-packaging technologies for optics chips (e.g., Si photonics) and high-performance large-scale integration (LSI) chips have attracted remarkable attention as they can considerably reduce the length of high-data-rate electrical links. For example, at OFC 2018, Rockley Photonics demonstrated a switch application specific integration circuit (ASIC) wherein Si photonics chips were co-packaged and a dozen ribbon optical fiber cables were connected to its package [2]. Such massively parallel optical input/output (I/O) connections are necessary for high-performance LSIs such as the upcoming high-capacity switch ASICs that are expected to have data transfer rates of over 100 Tbps.

Manuscript received 23 May 2022; revised 6 July 2022; accepted 8 July 2022. Date of publication 18 July 2022; date of current version 10 August 2022. This work was supported by the New Energy and Industrial Technology Development Organization (NEDO) under Grant JPNP13004. *(Corresponding author: Akihiro Noriki.)*

Akihiro Noriki, Satoshi Suda, and Takeru Amano are with the National Institute of Advanced Industrial Science and Technology (AIST), Tsukuba, Ibaraki 305-8568, Japan, and also with the Photonics Electronics Technology Research Association (PETRA), Tsukuba, Ibaraki 305-8569, Japan (e-mail: anoriki@aist.go.jp).

Isao Tamai, Yasuhiro Ibusuki, Akio Ukita, Koichi Takemura, Daisuke Shimura, Yosuke Onawa, and Hiroki Yaegashi are with the Photonics Electronics Technology Research Association (PETRA), Tsukuba, Ibaraki 305-8569, Japan.

Color versions of one or more figures in this letter are available at https://doi.org/10.1109/LPT.2022.3191645.

Digital Object Identifier 10.1109/LPT.2022.3191645

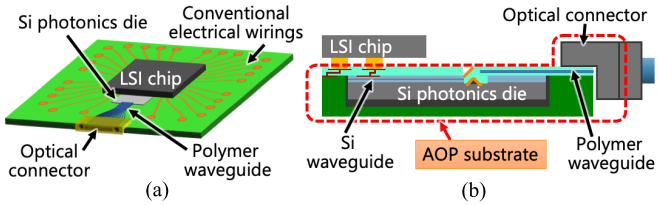

Fig. 1. (a) Bird's-eye view and (b) cross-section schematic of co-packaged optics using AOP substrate.

We previously proposed a new package substrate referred to as the active optical package (AOP) substrate, as a novel co-packaging solution. The bird's-eye view and cross-sectional schematic of the AOP substrate are shown in Fig. 1. The AOP substrate is based on conventional organic package substrates such as glass epoxy. In the package substrate, Si photonics dies are embedded as optical/electrical conversion devices. The electrical I/Os of the Si photonics dies are connected via thin-film metallization (electrical redistribution). Its optical I/Os are connected to standard single-mode fibers (SMFs) via optical redistribution, which is composed of polymer waveguides and micro mirrors, as shown in Fig. 1. The optical coupling between the polymer waveguides and SMFs is established by the optical connector, which is passively assembled at the edge of the package substrate [3], [4].

Implementing the AOP substrate eliminates the need for an accurate flip-chip bonding process of the Si photonics dies and active alignment of the optical fibers to the Si photonics dies. Instead, the Si photonics dies are embedded in the package substrate using a rough alignment process. Their electrical and optical redistributions are realized using photolithography. Therefore, extremely fine alignment is easily achievable for the Si photonics I/Os with a panel-level process. Optical redistribution allows for high-density Si photonics I/Os (e.g., 50-μ pitch) to be redistributed to low-density single-mode fiber interfaces (e.g., 250-μ pitch). Thus, small high-density Si photonics chips can be fabricated without the restriction due to low-density fiber interfaces. The optical redistribution also aggregates the optical I/Os of multiple Si photonics dies to one optical connector or vice-versa. Furthermore, optical redistribution facilitates the optical fibers to be placed far from the Si photonics dies. Therefore, Si photonics dies can be placed close to or underneath the LSI chips. The length of the electrical interconnects between them is minimal. Such ultra-short interconnects without wire-bondings and/or micro-bumps afford excellent electrical characteristics such as fan-out wafer-level packages or three-dimensional stack integration [5].

Recently, we presented a feasibility study of the AOP substrate and demonstrated optical redistribution on an Si photonics die [6]. The loss of the fabricated optical redistribution and its wavelength dependence was also reported. In this letter, additional measurement results of the polymer waveguide optical characteristics and mirror surface profiles are provided. On the basis of these findings, we present further detailed analysis of the measurement results concerning the optical redistribution.

II. Components for Optical Redistribution

Two components are required to realize optical redistribution. The first is an optical waveguide that can be integrated on the package substrate, and the second is a coupling structure between the optical waveguide and embedded Si photonics die. These components should have low dependency on the wavelength and polarization in the desired transmission wavelength range.

A polymer waveguide can be used as the optical waveguide. It can be fabricated by a low-temperature process. Therefore, it is suitable for fabrication as part of back-end processes. We used SUNCONNECT (Nissan Chemical Industries Ltd.), a polymer waveguide material, as the broadband waveguide material in the transmission wavelength range. As the polymer waveguides were connected to standard SMFs, their mode-field diameters (MFDs) must be comparable to those of the SMFs.

To connect the polymer and Si waveguides, a coupling structure based on two micro mirrors was used. It provided low wavelength and polarization-dependent optical coupling as compared with a grating coupler, which is a popular surface coupling device [7], [8]. As shown in Fig. 1, the light from the Si waveguide is output by the bottom-side mirror to the top side. Next, the light is reflected again by the top-side mirror to the polymer waveguide. The size (i.e., width and height) of the mirrors should be larger than the spot size of the optical beam between the polymer and Si waveguides for appropriate reflection. Because the MFD of the polymer waveguide was adjusted to that of the SMF, the spot-size diameter of the beam should be at least 10 μm. Therefore, the mirror size should be larger than 14 μm. The coupling of the Si and polymer waveguides also required the connection of mode-mismatched MFDs. The MFD of the Si waveguide was increased to approximately 3 μm upon using a Si inverse taper waveguide (a spot size converter (SSC)) at the end region of the Si waveguide. However, there was still a large MFD mismatch. To match the MFD of the Si and polymer waveguides, a curved concave mirror was used as the bottom-side mirror. Owing to the curved surface, the beam waist diameter of the light can be converted from 3 μm to 10 μm.

Thermal and mechanical tolerances of the optical redistribution based on the above-mentioned components should be considered for practical applications. In our previous work, sensitivity to thermal deformation was studied for the coupling structure and we showed that the structure had a high thermal tolerance [9]. Tolerance evaluation to the package warpage, especially to study a behavior of the embedded Si photonics dies, is one of the future works. If the Si photonics die and the package substrate are bent in the same way, the warpage will not cause critical problem since the coupling structure is a very small local structure (the area is approximately 50×50 μm2) while the package warpage is a very large global deformation. That is, the global warpage will cause negligible deformation in the local coupling structure. And the warpage of the polymer waveguide will not cause considerable bending loss.

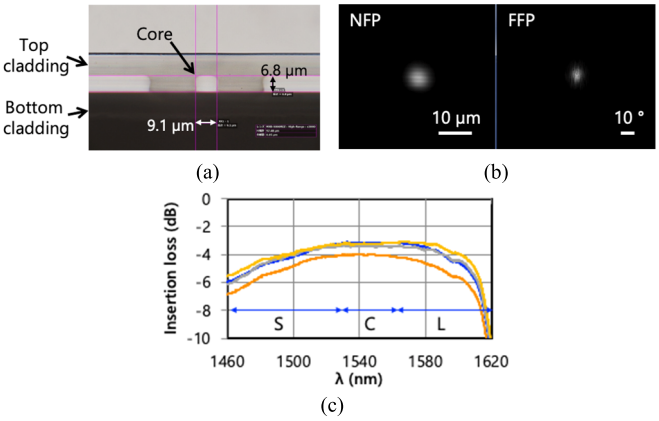

Fig. 2. (a) Cross-sectional optical microscopic image, (b) measured NFP and FFP, and (c) measured insertion loss spectrum of the fabricated polymer waveguides.

III. Fabrication

The fabrication process of optical redistribution on the Si photonics die was reported in detail in the previous report [6]. First, a cavity was formed on the surface of the Si photonics die to integrate a bottom-side mirror. Next, the mirror was fabricated by gray-scale lithography, as described previously [7], [8]. Then, the mirror was coated with a reflective metal layer and encapsulate by a transparent resin. Subsequently, a bottom cladding and core of the polymer waveguide were fabricated. Finally, the top-side mirror and top cladding were fabricated via the same gray-scale lithography process.

The polymer waveguides were fabricated to have an MFD, comparable to the standard SMF ($\sim$10 μm), by controlling its size and refractive index. A cross-sectional optical microscopic image of the polymer waveguide is shown in Fig. 2(a). The core width and height were 9.1 and 6.8 μm, respectively. The near-field pattern (NFP) and far-field pattern (FFP) are shown in Fig. 2(b). The NFP and FFP diameter were 7.8 μm and 12.4°, respectively, on average. Thus, the polymer waveguide had an MFD that was compatible with standard SMFs. The measured insertion loss spectrum of the 25-mm long polymer waveguide is shown in Fig. 2(c). As shown in the spectrum, the polymer waveguide has transparent broadband characteristics in the S, C, and L band. A coupling loss of $\sim$0.5 dB was estimated for the input and output facet. Therefore, the propagation loss was $\sim$1 dB/cm at a wavelength of 1550 nm.

Micro mirrors with a width and height of 20 and 14 μm, respectively, were fabricated using gray-scale lithography. Laser microscopic images and surface height profiles of the

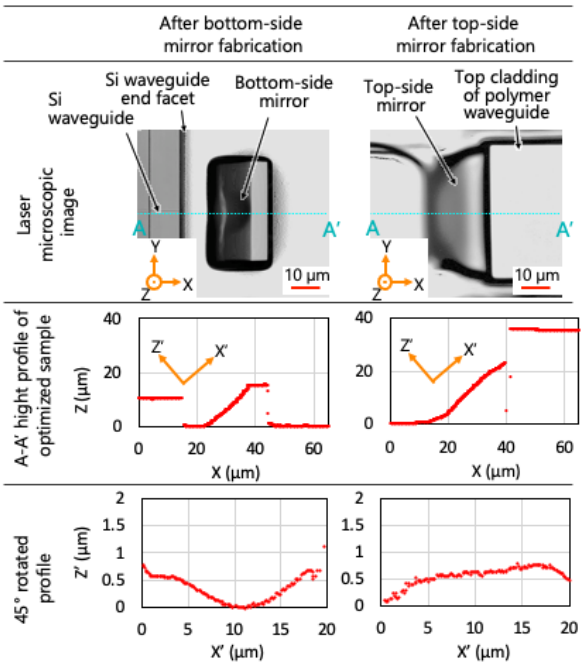

Fig. 3. Laser microscopic images, surface height profiles, and 45° rotated mirror surface profiles of the fabricated mirrors.

fabricated mirrors are shown in Fig. 3. The mirrors were sufficiently large to perfectly reflect the light beam with an MFD of 10 μm. To examine the detailed mirror surfaces, the 45° rotated profiles of the mirror surface are also shown in Fig. 3. Smooth mirror surfaces were obtained for the bottom and top-side mirrors. However, the profiles were slightly tilted so that the mirror angles were approximately 46°. There were some deformed areas in the mirror surfaces, particularly at the edges. This deformation induces stray light and leads to some optical loss. To generate the correct mirror angle, an auto-developer machine and a temperature-profile controllable hotplate chamber were used for stable baking and development processes. However, more careful controls of room temperature and humidity are necessary to stabilize the other processes like spin-coating.

The pitch of the fabricated optical redistribution was 100 μm. Reducing the pitch to 50 μm is possible with current design and fabrication technology. By modifying the mirror design and optimizing the fabrication technology, narrower pitch will be achieved. The minimum pitch will be approximately 20 μm since the mirror surface diameter over 14 μm is necessary for the standard-SMF-compatible polymer waveguide. If the pitch is narrow, cross talks of the polymer waveguides should also be considered. If the cross talk is critical, narrow-pitch polymer waveguide array can be fanned out to wide-pitch one immediately.

IV. Evaluation

The Si photonics die with optical redistribution was evaluated as a device-under-test (DUT) sample. The insertion loss spectrum of the DUT was measured in a wavelength range of the S, C, and L bands (1460–1620 nm), as shown in Fig. 4. Broadband light from a super luminescent diode

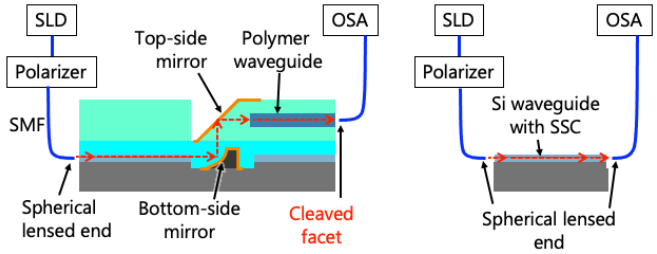

Fig. 4. Measurement setups for insertion loss of the DUT and reference samples. A spherical lensed fiber and standard SMF with cleaved end facet were used to receive the light from the Si and polymer waveguide, respectively, to match the MFD.

was polarized to TE polarization and provided as input to the Si waveguide end facet by using a spherical lensed fiber. The light was propagated via the Si waveguide, mirror-based coupling, and polymer waveguide. The light output from the polymer waveguide was received by a standard SMF with a cleaved end facet and measured by an optical spectrum analyzer (OSA). A spherical lensed fiber was used for the small-MFD Si waveguide and a cleaved facet SMF was used for the large-MFD polymer waveguide. To calculate the loss due to optical redistribution, the insertion loss of a Si photonics die without optical redistribution was measured as a reference sample. During reference measurement, another spherical lensed fiber was used to receive light output from the sample. Consequently, loss due to optical redistribution was derived by subtracting the insertion loss of the reference sample from that of the DUT. In this work, 1×8 splitter was integrated in the measured test pattern for measurement convenience. This splitter was not transparent in TM mode. Therefore, TM polarization was not evaluated. However, the optical redistribution composed of the mirror coupling and polymer waveguide can be low polarization dependent. The low polarization dependence of the bottom-side mirror was demonstrated in a previous work [8]. The top-side mirror will also be low polarization dependent of a few percent difference since it is a simple metallized planar mirror. The polymer waveguide was also low polarization dependent as reported in another previous work [10].

The measured loss spectrum of optical redistribution is shown in Fig. 5(a). It was measured on one single test pattern on one sample. The average loss was approximately 4 dB. The wavelength dependent loss was ± 1 dB except for the wavelength range over 1600 nm. As the optical redistribution was composed of a polymer waveguide and mirror-based optical coupling, the measured loss can be decomposed into the losses of these two components. On the basis of the measured propagation loss spectrum of the 25-mm long polymer waveguide (Fig. 2(c)), the estimation of the propagation loss of the 5-mm long polymer waveguide of the DUT is shown in Fig. 5(b). By subtracting the loss of the polymer waveguide propagation from that of the optical redistribution, the loss due to the optical coupling between Si and polymer waveguides was obtained, as shown in Fig. 5(c). Thus, it was revealed that the relatively large optical loss for the wavelength range over 1600 nm in Fig. 5(a) was from polymer waveguide characteristics. The coupling loss between Si and polymer waveguide

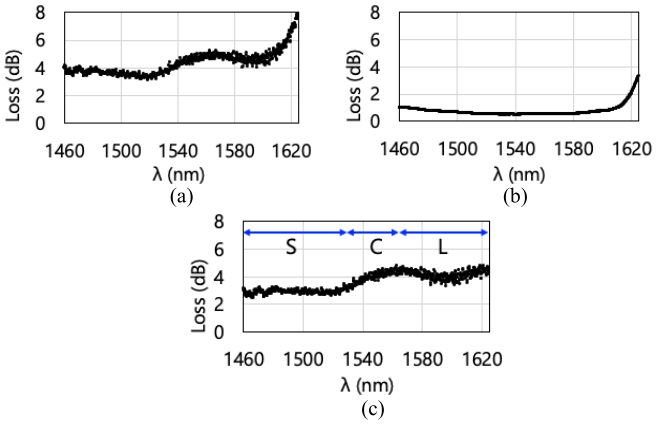

Fig. 5. (a) Measured loss spectrum of the optical redistribution. The loss can be decomposed into (b) polymer waveguide propagation loss and (c) mirror-based optical coupling loss.

was approximately 3.6 dB, and the wavelength dependent loss was ±0.65dB. Owing to the broadband characteristics of the mirror coupling, low wavelength dependent optical coupling was achieved for the Si waveguide and polymer waveguide connection. As described above, the mirror surface was sufficiently smooth to minimize light scattering, and the mirror surfaces were sufficiently large to perfectly reflect the light beam. However, deformations on the mirror surfaces led to the presence of some stray light. Therefore, the cause of the 3.6-dB coupling loss was concluded to be mode-mismatching loss, mis-alignment loss (including mirror angles), and optical loss of stray light which was caused by the deformed mirror surfaces.

To break down the 3.6-dB coupling loss, we prepared a simulation model of the fabricated structure and simulated the optical coupling efficiencies while optimizing the model parameters step by step. The simulation was performed using a physical optics propagation method presented in the commercial simulation software Zemax OpticStudio. Firstly, to evaluate the stray light loss, total incoming power to the polymer waveguide end facet was calculated. For the calculation, the power in a circle of 15-μm diameter, which was slightly larger than the size of the end facet, was integrated. The incoming power was 95%, so the stray light loss was 5%. Secondary, polymer-waveguide end-facet tilt angle was optimized in the model and the efficiency was improved by 32%. Thirdly, the end-facet position was optimized. The end facet was in de-focus position. By moving the end facet close to focus position, the efficiency was improved 19%. On the other hand, misalignment losses for the other two directions were small enough to be ignored. Thus, the misalignment loss was attributed from the de-focus condition. Finally, the MFD of the polymer waveguide was optimized and the efficiency was improved 37%. Remained 7% loss would be a part of the MFD mismatch loss and/or de-focus loss which cannot be optimized in the simulation. Thus, the tilt error, de-focus and MFD mismatch losses (32, 19 and 37%, respectively) were dominant factor. These losses can be decreased by optimizing the position, surface curvatures and tilt angle of the bottom side mirror. Using the initial prepared simulation model, the above three parameters were optimized. As the angle optimization, the x position of the top-side mirror was also tuned. As a result, the coupling efficiency of -0.7 dB was achieved in the simulation. Ultimately, the coupling efficiency of -0.4 dB was also achieved by using a planar top-side mirror which was not deformed.

V. Conclusion

The feasibility of optical redistribution, composed of two micro mirrors and a polymer waveguide, was studied on a Si photonics die. The fabricated optical redistribution loss was characterized. The average loss of approximately 4 dB and a wavelength dependent loss of ±1 dB were obtained for the wavelength range of 1460–1600 nm. The measured loss was decomposed into two loss factors, namely the polymer waveguide propagation loss and the coupling loss of Si and polymer waveguides via the two micro mirrors. The coupling loss was approximately 3.6 dB on average, and the wavelength dependent loss was ±0.65 dB over a 100-nm wavelength range. Thus, it was shown that the broadband optical redistribution was available based on mirror-based optical coupling and polymer waveguide. An advanced technology to integrate the optical redistribution on a glass epoxy substrate, in which the Si photonics die is embedded, will be developed in future works.

References

[1] R. Dangel *et al.*, "Polymer waveguides for electro-optical integration in data centers and high-performance computers," *Opt. Exp.*, vol. 23, no. 4, pp. 4736–4750, 2015, doi: 10.1364/OE.23.004736.

[2] (2018). *Rockley Photonics Showcases Its in-Packaged Design at OFC*. Gazettabyte. [Online]. Available: http://www.gazettabyte.com/home/2018/3/15/rockley-photonicsshowcases-its-in-packaged-design-at-ofc.html

[3] A. Noriki *et al.*, "Low-cost MT-ferrule-compatible optical connector for co-packaged optics using single-mode polymer wave guide," in *Proc. IEEE 69th ECTC*, May 2019, pp. 2042–2047.

[4] A. Noriki *et al.*, "MT-ferrule compatible passive optical coupling for single-mode polymer wave guide in co-packaged optics," *Proc. SPIE*, vol. 11286, pp. 80– 85, Feb. 2020, doi: 10.1117/12.2547051.

[5] P. Wesling, Ed., *Heterogeneous Integration Road Map (HIR)*. Accessed: May 16, 2022. [Online]. Available: https://eps.ieee.org/images/files/HIR_2020/ch21_sip-module.pdf

[6] A. Noriki *et al.*, "Demonstration of optical re-distribution on silicon photonics die using polymer wave guide and micro mirrors," in *Proc. Eur. Conf. Opt. Commun. (ECOC)*, 2020, pp. 1–4, doi: 10.1109/ECOC48923.2020.9333180.

[7] A. Noriki *et al.*, "45-degree curved micro-mirror for vertical optical I/O of silicon photonics chip," *Opt. Exp.*, vol. 27, no. 14, pp. 19749–19757, 2019, doi: 10.1364/OE.27.019749.

[8] A. Noriki *et al.*, "Mirror-based broadband silicon-photonics vertical I/O with coupling efficiency enhancement for standard single-mode fiber," *J. Lightw. Technol.*, vol. 38, no. 12, pp. 3147–3155, Jun. 15, 2020, doi: 10.1109/JLT.2020.2995915.

[9] F. Nakamura *et al.*, "Analyzing thermal tolerance of mirror-based optical redistribution for co-packaged optics," in *Proc. Conf. Lasers Electro-Optics (CLEO)*, 2022, Paper SF3O.8.

[10] S. Suda *et al.*, "Transmission of 43-Gb/s optical signals through a single-mode polymer waveguide for LAN-WDM," *Proc. SPIE*, vol. 11277, pp. 49–54, Mar. 2020, doi: 10.1117/12.2544202.